REPORT DOCUMENTATION PAGE

AFRL-SR-BL-TR-01-

0651

1. AGENCY USE ONLY *(Leave blank)*	2. REPORT DATE	3. REPORT TYPE AND DATES COVERED
		FINAL (01 AUG 97 TO 31 JUL 98)

4. TITLE AND SUBTITLE
MECHANISM BASED FAILURE LAWS FOR GRAPHITE/EPOXY COMPOSITES

5. FUNDING NUMBERS
F49620-97-1-0450

6. AUTHOR(S)
VIJAY GUPTA

7. PERFORMING ORGANIZATION NAME(S) AND ADDRESS(ES)
DEPARTMENT OF MECHANICAL AND AEROSPACE ENGINEERING
UNIVERSITY OF CALIFORNIA, LOS ANGELES

8. PERFORMING ORGANIZATION REPORT NUMBER

9. SPONSORING/MONITORING AGENCY NAME(S) AND ADDRESS(ES)
AFOSR/NA
801 N. RANDOLPH STREET
ROOM 732
ARLINGTON, VA 22203

10. SPONSORING/MONITORING AGENCY REPORT NUMBER

11. SUPPLEMENTARY NOTES

12a. DISTRIBUTION AVAILABILITY STATEMENT

12b. DISTRIBUTION CODE

13. ABSTRACT *(Maximum 200 words)*

A significant progress has been made towards achieving the overall goal of developing mechanism-based failure laws for graphite/epoxy laminate under biaxial compression. Microstructural-level mechanisms have been largely uncovered using examination of load-interrupted specimens, including the strength data under different materials axes orientations and in-plane biaxiality ratios. Mechanism-based failure laws for uniaxial compression have also been developed, including a fracture mechanics-based predictive crack density model. New and unusual size effects related to modulus were uncovered, and so were the observations that seem to indicate fiver microbuckling mechanism to be simply end loading related.

20020107 091

14. SUBJECT TERMS

15. NUMBER OF PAGES
13

16. PRICE CODE

17. SECURITY CLASSIFICATION OF REPORT	18. SECURITY CLASSIFICATION OF THIS PAGE	19. SECURITY CLASSIFICATION OF ABSTRACT	20. LIMITATION OF ABSTRACT
UNCLASSIFIED	UNCLASSIFIED	UNCLASSIFIED	

MECHANISM BASED FAILURE LAWS FOR GRAPHITE/EPOXY COMPOSITES

F49620-97-1-0450

Vijay Gupta
Department of Mechanical and Aerospace Engineering
University of California, Los Angeles

2. Objectives

No change in the objectives, which was to develop mechanism-based failure laws for graphite/epoxy laminates under biaxial compression.

3. Status of Effort

A significant progress has been made towards achieving the overall goal of developing mechanism-based failure laws for graphite/epoxy laminates under biaxial compression. Microstructural-level mechanisms have been largely uncovered using examination of load interrupted specimens, including the strength data under different material axes orientations and in-plane biaxiality ratios. Mechanism-based failure laws for uniaxial compression have also been developed, including a fracture mechanics-based predictive crack density model. New and unusual size effects related to modulus were uncovered, and so were the observations that seem to indicate fiber microbuckling mechanism to be simply end loading related.

4. Accomplishments/New Findings

Overall Effort

The failure mechanisms and stress-strain behavior have been investigated for different geometries and fiber orientations of graphite-epoxy (AS4/3502 and IM7/8551-7) laminates under off-axis uniaxial and biaxial compression. Samples with different aspect ratios and fiber orientations were tested to evaluate the different modes of failure and investigate size effects related to the laminate strength and stiffness. Figure 1 shows the geometry of the tested specimens, indicating how changing the specimen size for fixed ply orientation allowed investigating the influence of the amount of constrained (loading ends) vs. the unconstrained (by side faces) fibers. In-plane biaxial testing was also conducted with varying confinement ratios in order to identify the failure mechanisms and stress-strain behavior under various stress states. Results from these investigations were used to develop fracture mechanics-based failure criteria for the laminates. For the purpose of brevity, only results for the AS4/3502 are presented here. The results for the IM7/8551-7 system parallel those of the AS4/3502 system but with a much larger capacity to accommodate damage. Also the strain and the confinement ratio at which the transition from ductile (crack-induced) to brittle behavior was observed was higher for the IM7/8551-7 system.

New Findings-Failure Mechanisms

To accomplish the main goal of developing mechanism-based failure laws under biaxial compression, the microstructural-level crack nucleation and propagation events were recorded by sectioning samples recovered from tests interrupted at different stages of loading. For this study, $[0]_{48}$, $[\pm10]_{12s}$, $[\pm15]_{12s}$, $[\pm30]_{12s}$, $[\pm45]_{12s}$ and $[90]_{48}$ specimens,

with various aspect ratios (height/width) were tested with an end loading fixture. Failure modes varied depending on the fiber orientation of the laminate layers to the loading axis. Failure transitioned from shear slipping along the fibers in the $[\pm 45]_{12s}$ and $[\pm 30]_{12s}$ samples to global delamination in the $[\pm 10]_{12s}$ samples. Figure 2 shows the event of shear crack nucleation in the $[\pm 45]_{12s}$ sample matrix, just after the peak stress. This led to a small decrement in the stress, which remained essentially constant thereafter (Fig. 4). This plateau region was characterized by the formation of longitudinal cracks aligned with the fiber axis, and appeared as transverse cracks on the specimen sides. Each of these cracks were associated with two ply debond cracks that nucleated from their tips in order to accommodate the strain incompatibility generated by crack face sliding of the longitudinal crack. The longitudinal main crack and its two "wings" in the form of ply debond cracks nucleated in a pair, with the unit stabilizing after the arrest of the ply debond cracks at the interply boundary. The length of the plateau region was dictated by the saturation of the transverse cracks throughout the sample and ultimately led to specimen failure by delamination. Figure 3 shows the side view of a sample after it had attained the saturation cracking state. The source of the delamination was traced to the unstable propagation of the ply debond cracks.

The $[\pm 30]_{12s}$ samples failed in a brittle fashion on a single shear fault plane, without any plateau region in the stress-strain behavior. The trend of increasing brittleness with decreasing fiber orientation continued, such that for the $[\pm 10]_{12s}$ samples, the failure was catastrophic and characterized by global delaminations aligned with the load axis. In carefully conducted experiments, the source of the delamination was traced to the deflection of in-plane matrix shear cracks at the interply boundaries. Micromechanics-based models were used to rule out failure due to interlaminar shearing and across ply tensile stress-induced delaminations. The calculation of the relevant stresses associated with the latter two mechanisms were based on a beam-on-elastic foundation model using the ply and the in-plane and out-of-plane fiber waviness from experiments as an input. Similarly interlaminar matrix shearing due to fiber scissoring was found not to be the source of these delaminations.

The 0° samples were found to delaminate. Fiber kinking was found not to be the strength-limiting mechanism. It appears that both the fiber kinking and matrix-shear-induced axial delaminations are essentially end-loading-related mechanisms in that end-gripped samples display the former mechanism while the latter governs failure when loaded directly through a plate. Rather interestingly, and also fortunately, the ultimate compressive strength for both these mechanisms turns out to be quite close for the present materials. Nevertheless one should be cognizant of the above facts especially if the design is based on failure mechanism and not ultimate strength. Additional experiments are presently being carried out to further confirm the above, by changing the specimen end conditions using double-sided tapes and epoxies of different shear strengths to glue the specimen ends to the loading platens.

Biaxial compression testing was also conducted on $[\pm 30]_{12s}$ and $[\pm 45]_{12s}$ samples with a cruciform material testing machine. Samples were loaded along two axes with platens slightly smaller than the sample widths (Figure 5). The confinement ratio R, the ratio of stress applied to the secondary to primary sample axes, was varied from 0.24 to

arly 1 to measure the sensitivity of sample failure mechanisms and stress-strain havior (Fig. 6) to different stress states. Failure modes for both fiber orientations nsitioned from the uniaxial failure mode to massive delamination with an increasing nfinement ratio. The source of these delaminations was conclusively traced to angled atrix shear cracks formed between the two plies due to the out-of-plane shear stress. he traces of few of these cracks which did not become unstable could be seen on the side faces of the sample, with their planes inclined at more of less 45° to the loading axis and their tips resting on the adjacent plies. Figure 7 shows examples of such cracks. The other cracks which became unstable did so by generating what are called "wing cracks" from their tips and realized as delaminations on the global specimen scale. This deformation feature was identical to all 45° and 30° samples under high confinement ratios.

The increased biaxial loading also increased the specimen stiffness and strength.

The results for the IM7/8551-7 system were found to parallel those of the AS4/3502 system but with a much larger capacity to accommodate damage. Also the strain and the confinement ratio at which the transition from ductile (crack-induced) to brittle behavior was observed was higher for the IM7/8551-7 system.

These investigations led to further understanding of the coupling between failure modes and the influence of constituent stresses under various applied stress states to develop analytical failure models, a task which is presently in progress.

New Findings-Size Effects on Strength and Stiffness

The stress-strain data for each orientation was found to be strongly specimen-size-dependent. Irrespective of the fiber orientation, the elastic modulus showed a rather counterintuitive trend, namely, it increased with the specimen height and aspect ratio (Fig. 8)! Thus, short samples appeared more compliant than the taller ones having identical fiber orientation. The variation in the stress-strain curve slopes for 8 to 10 samples with the same height was small enough and did not pervade in the next data set for the samples with different heights. A systematic study carried out on two different machines ruled out the effect of the loading apparatus, and also of the end-loading-related mechanisms of fiber bending and scissoring in short samples where the two fiber ends exited the loading ends. Also since specimens of the various sizes were cut from the same laminate for each angle cross-ply orientation, differences due to laminate-to-laminate variability could also be ruled out. After an in-depth investigation, using strain gauge-measured data over the specimen surfaces, this counterintuitive effect was found to be real and the increased compliance of the shorter samples was attributed to frictional sliding of the sample's loading ends in the thickness direction.

Figure 9 shows the variation in the measured peak stress for each orientation as a function of the specimen height and aspect ratio. These figures suggest the ultimate strength to be inversely proportional to these variables. This is expected based on the Weibull-type statistics where taller samples have a higher probability of strength-

degrading defects, which in these specimens, were interply voids generated during the hot pressing stage of sample manufacturing. Rather interestingly, such a data set rules out the possibility of end-loading related premature failure in fully constrained short samples where one would have expected lower strengths compared to the unconstrained set on account of increased ply bending and fiber scissoring.

The above results on strength and stiffness highlight the importance of specimen geometry and fixturing considerations for off-axis compression testing and the sensitivity of stress-strain behavior to specimen size. Gathering and understanding of such a data set is important for realizing the widespread use of graphite/epoxy laminates in aerospace and civil infrastructure applications. Additionally, such a study allows transferring the laboratory data from small test coupons to larger structures in service. All this is in line with the Airforce's mission of developing high performance lightweight structures.

5. Personnel Supported

Vijay Gupta, Principal Investigator
Serge Hauert-Graduate Student
Dan Potter-Graduate Student who received his MS degree under this grant in June 1998.

6. Publications

Refereed Journal Articles

1. The Effect of Specimen Size and Aspect Ratio on the Compressive Strength of Graphite/Epoxy Laminates, Dan Potter, Vijay Gupta, and Serge Hauert, Submitted to *Comp. Sci. Technology*, 1999.

2. The Effect of Specimen Size and Aspect Ratio on the Elastic Stiffness of Graphite/Epoxy Laminates, Dan Potter, Vijay Gupta, and Serge Hauert, Submitted to *Comp. Sci. Technology*, 1999.

3. Mechanism-based Modeling of Compressively-Loaded Graphite/Epoxy Laminates, Serge Hauert, Vijay Gupta, and Dan Potter, Submitted to *Comp. Sci. Technology*, 1999.

4. Measurement of the in-situ Fiber/Matrix Interface Strength in Graphite/Epoxy Composites," A. Yu and V. Gupta, Composites Science and Technology, in press.

7. Seminar/Presentations/Conference Proceeding Papers

1. Biaxial Failure Mechanisms, presented at the Meeting of the 12th U.S. National Congress of Theoretical and Applied Mechanics held in Florida, 1998.

2. Failure Mechanisms and Size Effects in Graphite/Epoxy Laminates under Off-axis Uniaxial and Biaxial Compression, presented and appeared in the Proceedings of the Fifth International Conference on Composite Engineering, D. Hui, ed., pp. 347-348, July 1998

3. A presentation encompassing the above observations were made at the AFOSR Mechanics of Composite Materials Program Review in Dayton, OH, Oct. 14-16, 1998.

4. Three papers were presented at the Winter Annual Meeting of the ASME held in Anaheim, CA, November 15-20, 1998:

(a) Failure Mechanisms under Uniaxial Compression, in the Symposium on Life Prediction of Materials and Structures. The paper also appeared in an abstract book.

(b) Size Effect in Strength and Stiffness of Laminates, in the Symposium on Micromechanics and Laminate Analysis in honor of the 65th Birthday of Dr. Pagano, and

(c) Failure Mechanisms under Biaxial Compression, in the Symposium on Micromechanical Failure in Composites.

5. Micromecahnical Modeling of Laminates under Biaxial Compression, presented at the PACAM VI meeting held in Rio de Janerio, Brazil, Jan2-8, 1999.

8. New Discoveries, inventions, patent disclosures-none

9. Honor/Awards-none

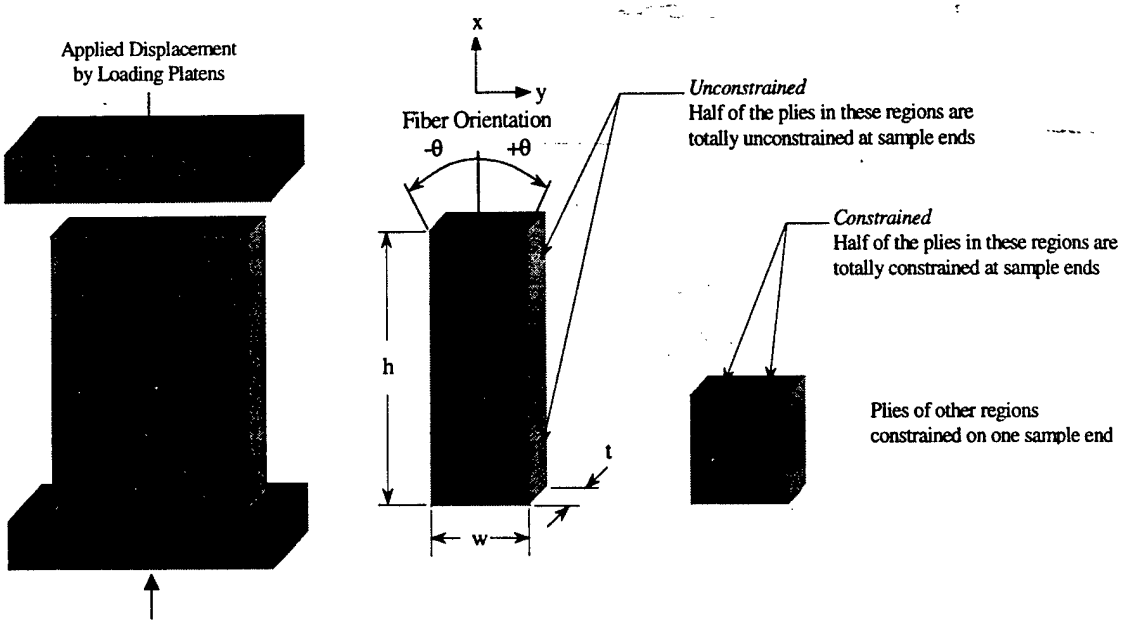

h=33 mm
w=25 mm
t=6 mm

h=33 mm
w=13 mm
t=6 mm

h=13 mm
w=13 mm
t=6 mm

Figure 1

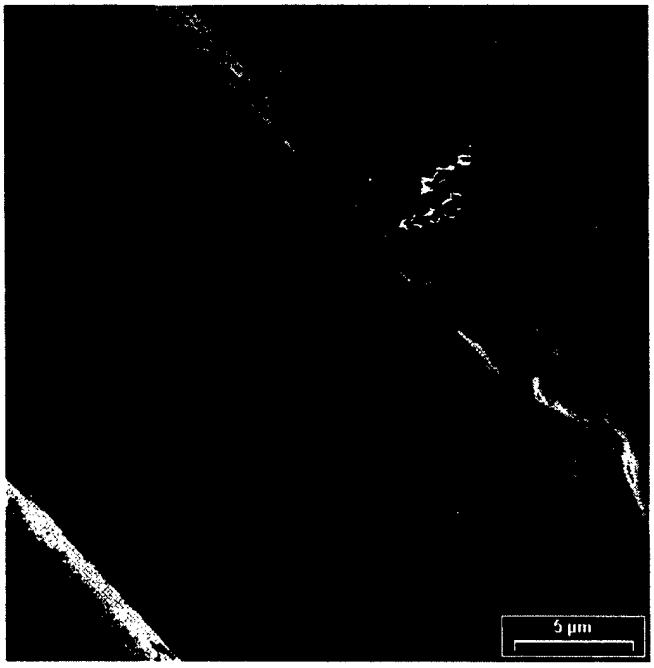

Figure 2

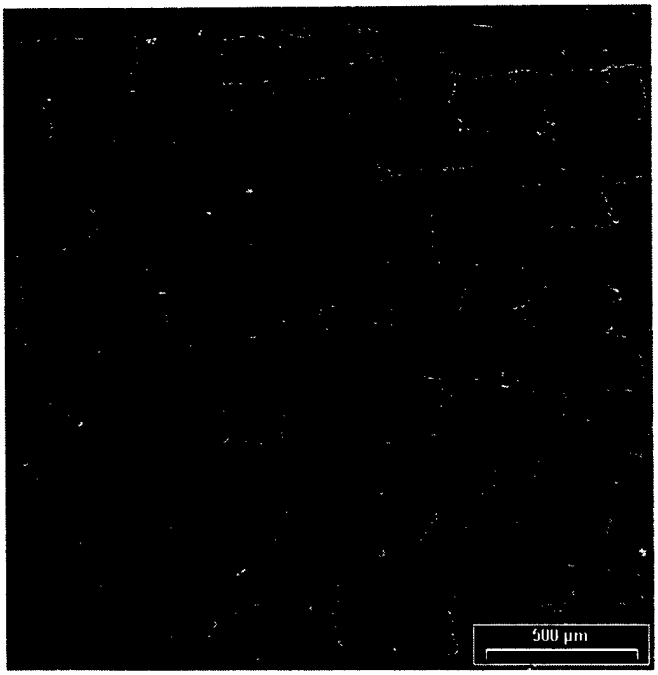

Figure 3

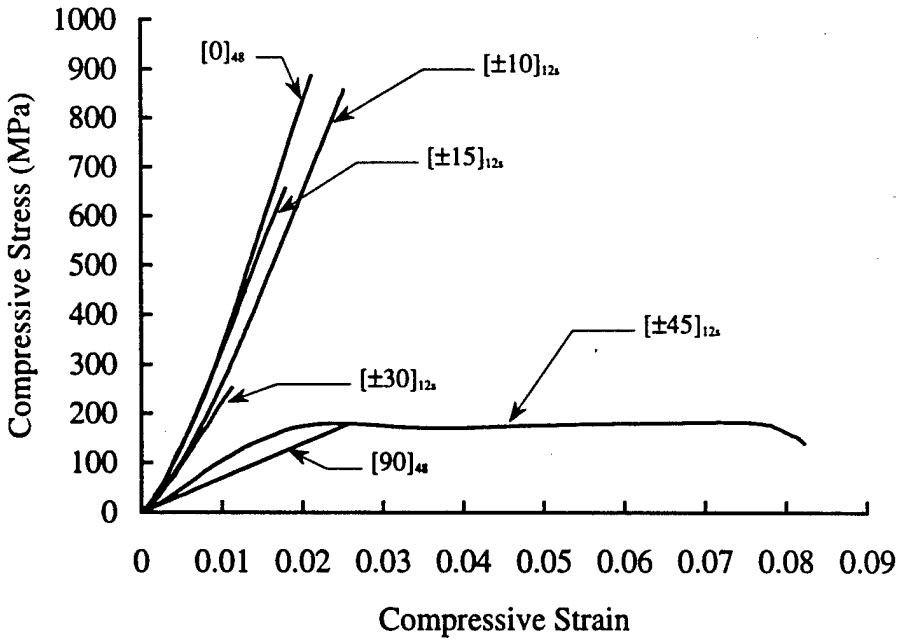

Figure 4

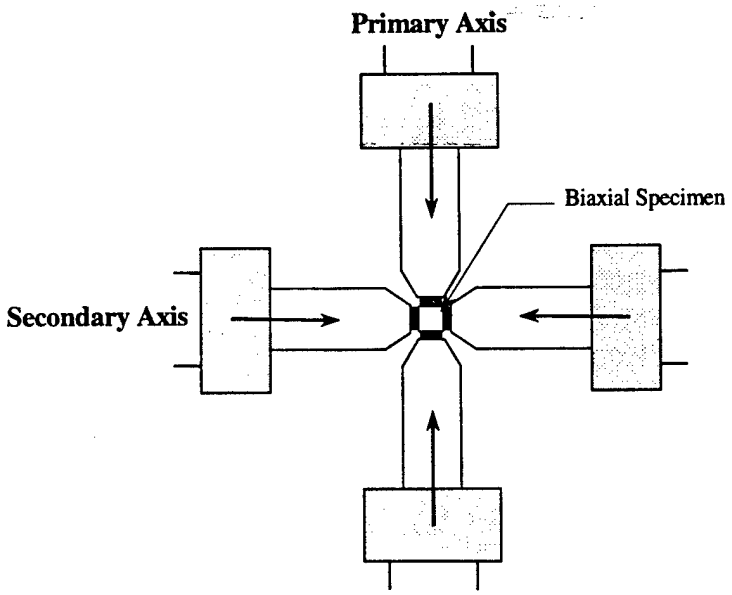

Figure 5

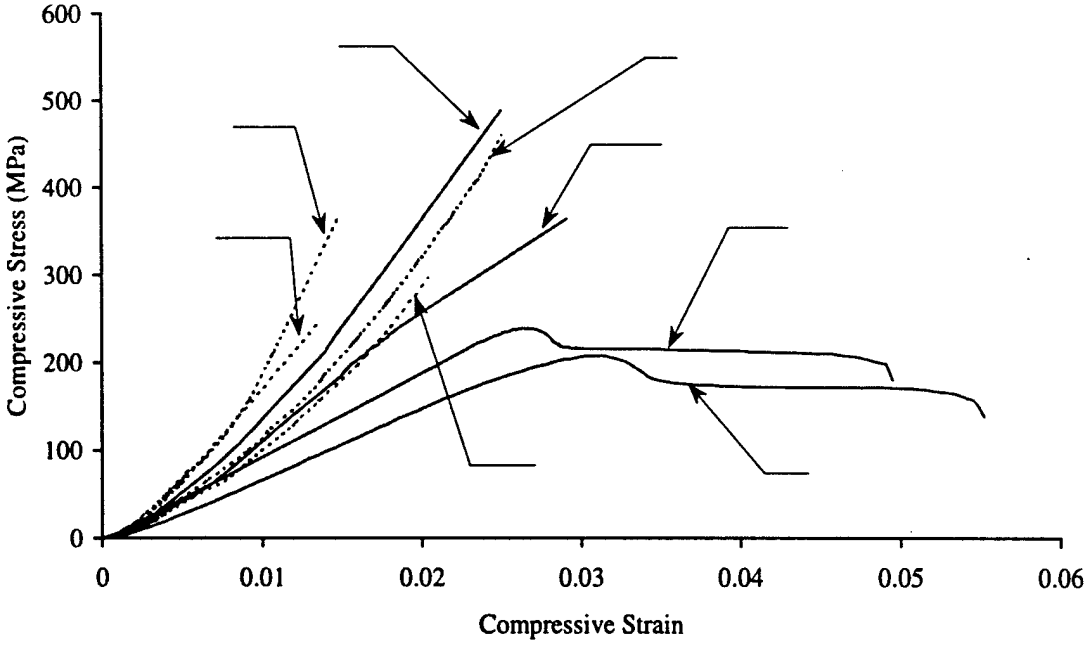

Figure 6

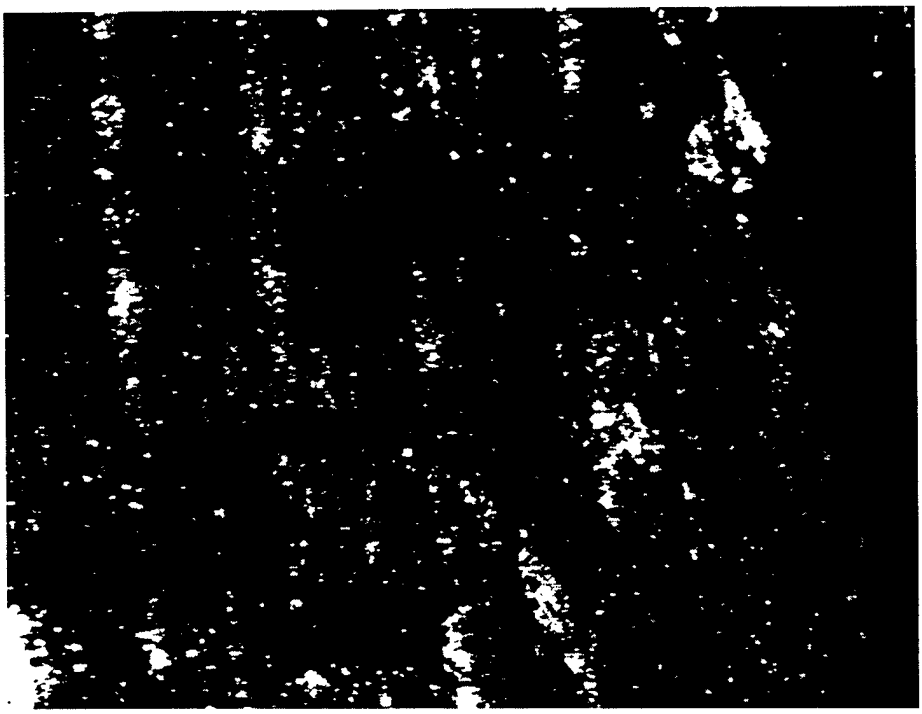

Figure 7

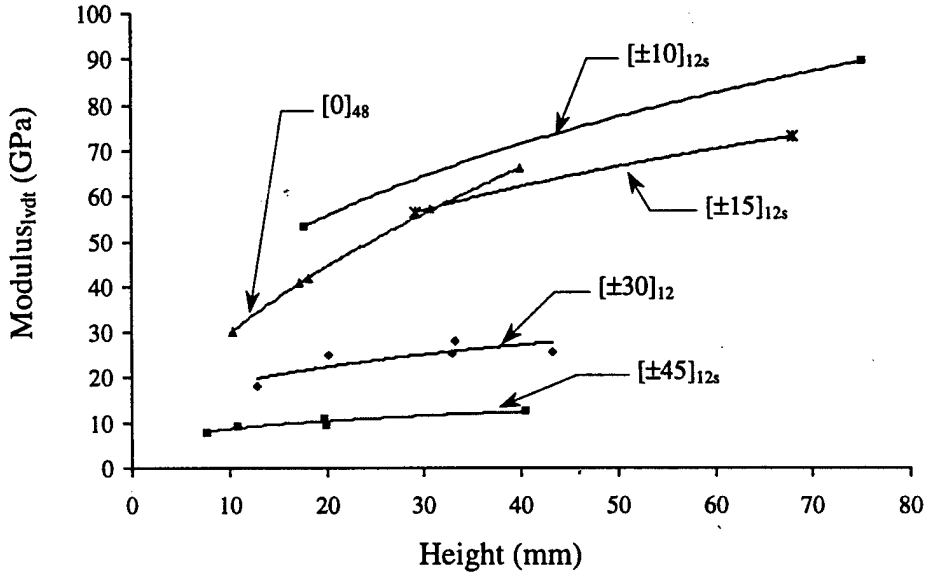

Fig. 8a Modulus$_{lvdt}$ vs. Height

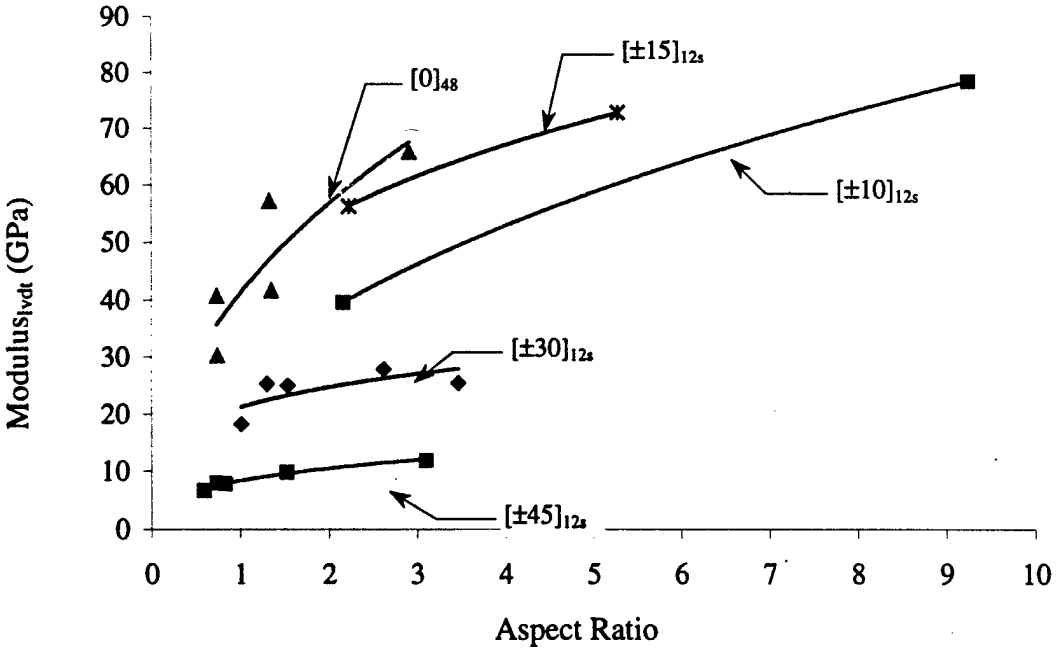

Fig. 8b. Modulus$_{lvdt}$ vs. Aspect Ratio

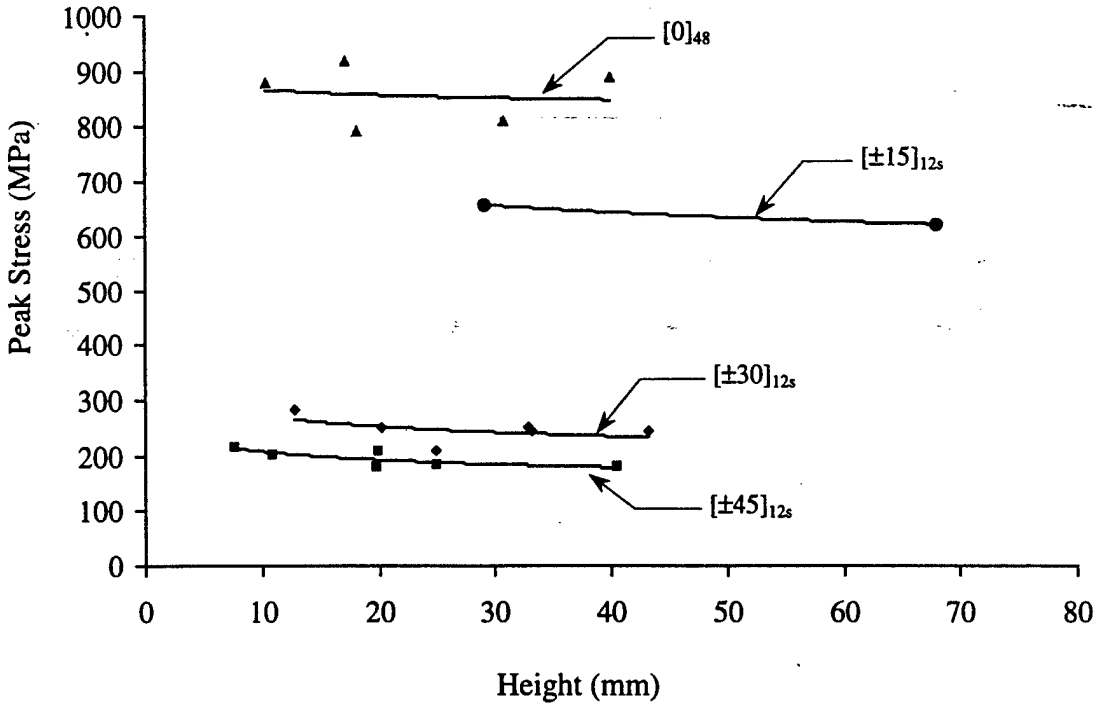

Fig. 9a Peak Stress vs. Height

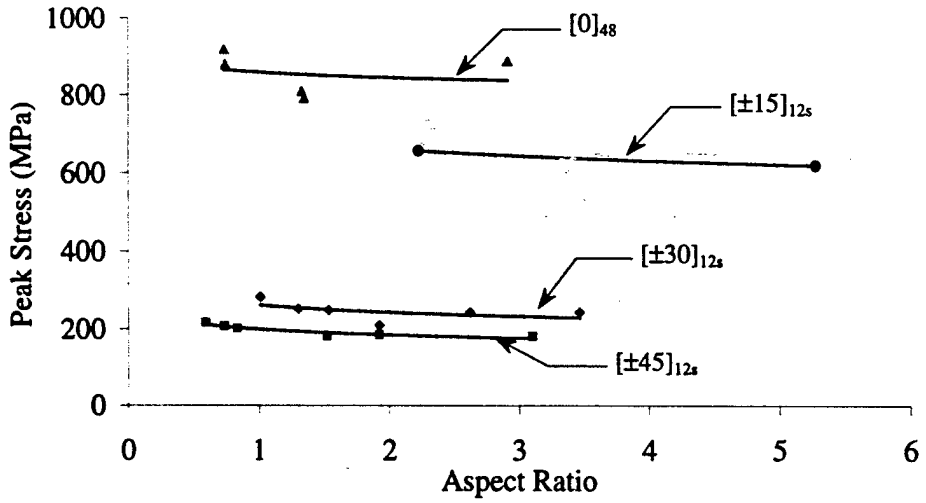

Fig. 9b. Peak Stress vs. Aspect Ratio